Journal of Power Sources 192 (2009) 573–581

Contents lists available at ScienceDirect

Journal of Power Sources

journal homepage: www.elsevier.com/locate/jpowsour

On-board hydrogen storage and production: An application of ammonia electrolysis

Bryan K. Boggs, Gerardine G. Botte*

Department of Chemical Engineering, 183 Stocker Center, Ohio University, Athens, OH 45701, USA

ARTICLE INFO

Article history:
Received 18 February 2009
Received in revised form 5 March 2009
Accepted 5 March 2009
Available online 19 March 2009

Keywords:
Ammonia electrolysis
Ammonia electrolytic cell
On-board hydrogen production
Hydrogen storage
Fuel cells

ABSTRACT

On-board hydrogen storage and production via ammonia electrolysis was evaluated to determine whether the process was feasible using galvanostatic studies between an ammonia electrolytic cell (AEC) and a breathable proton exchange membrane fuel cell (PEMFC). Hydrogen-dense liquid ammonia stored at ambient temperature and pressure is an excellent source for hydrogen storage. This hydrogen is released from ammonia through electrolysis, which theoretically consumes 95% less energy than water electrolysis; 1.55 Wh g^{-1} H_2 is required for ammonia electrolysis and 33 Wh g^{-1} H_2 for water electrolysis. An ammonia electrolytic cell (AEC), comprised of carbon fiber paper (CFP) electrodes supported by Ti foil and deposited with Pt–Ir, was designed and constructed for electrolyzing an alkaline ammonia solution. Hydrogen from the cathode compartment of the AEC was fed to a polymer exchange membrane fuel cell (PEMFC). In terms of electric energy, input to the AEC was less than the output from the PEMFC yielding net electrical energies as high as 9.7 ± 1.1 Wh g^{-1} H_2 while maintaining H_2 production equivalent to consumption.

1. Introduction

1.1. On-board hydrogen production

Interest in hydrogen fuel-cell vehicles (HFCVs) has been increasing in popularity over the past decade. This is primarily a result of the shrinking oil reserves which are expected to last only 42 years as of 1998 [1]. HFCVs have also found a niche in the environmental and political fields because they offer a solution for eliminating the harmful air pollutants generated by internal combustion engines (ICEs) such as nitrogen oxides (NO_x), volatile organic compounds (VOCs), carbon dioxide (CO_2), and sulfur dioxide (SO_2) [2–4]. In addition to being environmentally friendly, HFCVs are quiet and convert 50–60% of the energy available in hydrogen to power the automobile rather than the 20–30% efficiency of today's hydrocarbon-dependent vehicles [5,6].

A hydrogen future is not only driven by the transportation sector but as a movement for reducing oil imports in general and eliminating the dependence on petroleum for daily energy production. HFCVs as personal transportation vehicles are believed to be the best alternative. They have high efficiencies, emit no harmful pollutants, and can operate in cold temperatures unlike battery-powered vehicles (BPVs) [7,8]. However, storing enough hydrogen that allows a fuel-cell vehicle to travel the same range as today's ICEs between refueling is proving difficult and delaying the commercialization and market approval of HFCVs. Compared to gasoline, hydrogen has 2.7 times more energy content based on weight. However, due to its tremendously low density, hydrogen has 25% less energy content than gasoline when based on volume [9]. Because of this, there is no storage technology currently available that allows a vehicle to travel the average 482-km range that today's internal combustion engines obtain [10].

As a result, research on producing hydrogen on board has accelerated. Generating hydrogen on board in a manner that does not produce air pollutants and requires the small amount of energy available from renewable sources is the definite long-term solution [3]. This is where *in situ* ammonia electrolysis enters the picture.

1.2. Ammonia and electrolysis

Liquid ammonia is a non-carbon containing hydrogen-dense (17.6 wt.%) fuel that can be stored at ambient temperature and pressure [11]. Theoretically, ammonia electrolysis requires 95% less energy than water electrolysis (1.55 Wh g^{-1} H_2 versus 33 Wh g^{-1} H_2). In fact, Vitse et al. state that hydrogen produced from the electrolysis of ammonia costs 0.89 US$ kg^{-1} of H_2 opposed to 7.10 US$ kg^{-1} of H_2 from water electrolysis. These numbers were based on an ammonia cost of 275 US$ ton^{-1} and a solar energy cost of 0.214 US$ kWh^{-1} [12]. This low cost is single-handedly a result of the low energy consumption of ammonia electrolysis. The

* Corresponding author. Tel.: +1 740 593 9670; fax: +1 740 593 0873.
E-mail address: botte@ohio.edu (G.G. Botte).

0378-7753/$ – see front matter © 2009 Elsevier B.V. All rights reserved.
doi:10.1016/j.jpowsour.2009.03.018

U.S. Department of Energy's (DOE's) targeted cost of hydrogen for 2015, per kg of hydrogen or gallon of gasoline equivalent (gge), is US$ 2–3 [10]. Ammonia electrolysis has other uses besides generating hydrogen for mobile applications such as nitrate desalination at domestic wastewater treatment plants, electrochemical sensors, and for the production of nitrogen [12–14].

$$2NH_3(aq) + 6OH^- \rightarrow N_2(g) + 6H_2O + 6e^- \quad (1)$$

$$6H_2O + 6e^- \rightarrow 3H_2(g) + 6OH^- \quad (2)$$

$$2NH_3(aq) \rightarrow N_2(g) + 3H_2(g) \quad (3)$$

At the anode (Eq. (1)), ammonia is electro-oxidized and has a potential of −0.77 V versus standard hydrogen electrode (SHE). Alkaline reduction of water occurs on the cathode and requires −0.83 V versus SHE. Overall, Eq. (3), 0.06 V are required. This makes ammonia electrolysis attractive for producing hydrogen when comparing the required 1.23 V for water electrolysis according to the thermodynamics at standard conditions [12].

There is criticism when discussing the possibilities of using ammonia as a source of hydrogen storage that is echoed in the DOE position paper that discusses the use of ammonia for onboard storage. This DOE paper only discusses the feasibility of ammonia thermal cracking rather than other novel ammonia–hydrogen technologies such as electrolysis. Cracking ammonia requires temperatures greater than 500 °C, ammonia purification equipment to prevent ammonia poisoning of fuel cells, and a complex system [11]. Alkaline fuel cells (AFCs) could use the ammonia-doped hydrogen reducing the threat of poisoning, but these fuel cells require operating temperatures ranging from 65 to 220 °C [15]; as a result, the overall energy requirements increase. On the other hand, ammonia electrolysis and the hydrogen–air polymer exchange membrane fuel cell (PEMFC) process requires ambient temperature and pressure. Also, little or no ammonia purification equipment for the fuel cell is required because the cathode side of the AEC (where H_2 is generated) only needs to be in contact with KOH.

Another criticism is the availability of ammonia. According to the DOE, ammonia has been produced for more than 100 years economically using the Haber–Bosch process. Also, there are more than 4800 km of ammonia distribution pipelines that spreads over much of central U.S. allowing distribution costs of ammonia to be similar to liquid petroleum gasoline (LPG) distribution costs [11]. Even more convincing, nearly 54 million metric tons of gas-phase ammonia is emitted into the atmosphere world wide annually. Major sources include domestic animal excreta (40.2%), synthetic fertilizers (16.7%), oceans (15.2%), burning of biomass (10.9%), crops (6.7%), human excreta (4.8%), soils under vegetation (4.4%), and industrial processes (0.6%) [16]. It is safe to assume, especially for the excreta sources, that the liquid-phase ammonia, which is generating much of the gas, is higher in concentration. According to McCubbin et al., gas-phase ammonia emissions contribute to the formation of ammonium nitrate and sulfate. They found that these particulate emissions can result in a variety of health problems including: asthma attacks, chronic bronchitis, and even premature mortality and suggested that a 10% reduction in ammonia emissions would save US$ 4 billion in health costs each year [17]. Moreover, nitrate contamination of groundwater is largely due to liquid-phase ammonia emissions from both human and animal excreta. Too much exposure to nitrates can lead to methemoglobinemia, which prevents the transport of oxygen by the blood. As a result, the U.S. Environmental Protection Agency (EPA) has limited the nitrate contamination level in drinking water to 10 mg L^{-1}. This is believed to be a pandemic and remediation costs are high [18].

Talini and coworkers [19] has demonstrated that 97% of ammonia present in urine can be captured through stripping and absorption. Even more promising, urea present in urine is easily hydrolyzed to ammonium increasing the amount of ammonia present in urine. Moreover, naturally occurring enzymes called urease decomposes urea to ammonia by the following reaction [20]:

$$NH_2(CO)NH_2 + 2H_2O \rightarrow NH_3 + NH_4^+ + HCO_3^- \quad (4)$$

Utilizing this free ammonia as hydrogen storage, results in an estimated 0.33 US$ kg^{-1} of H_2 theoretically; this does not include the stripping and absorption equipment used to capture the ammonia. Essentially, ammonia can be called a biofuel. It is difficult to compare to other biofuels such as ethanol because the sewer-to-ammonia-to-wheel efficiency is much higher than the ammonia-to-fertilizer-to-corn-to-ethanol-to-wheel cycle that ethanol faces. Plus, ethanol-combusting vehicles emit the same air pollutants as today's automobiles and depend heavily on climate conditions [21].

Thermodynamically for 1 g of H_2, ammonia electrolysis consumes 1.55 Wh. For this same gram of H_2, a PEMFC, which is the reverse reaction of water electrolysis, generates 33 Wh. After sending 1.55 Wh back to the AEC from the PEMFC, making the system self sustaining, there is potential for a net energy of 31.45 Wh that can be used to recharge the batteries used for system start-up, to power a motor, or for any other applications. However, PEMFCs have efficiencies that range from 50 to 60% [5,6]. Additionally, ammonia is converted to hydrogen with 100% Faradaic efficiency, but kinetic problems creating large ammonia oxidation overpotentials exist [12].

The focus of this paper is on-board hydrogen production with *in situ* ammonia electrolysis. The goal is to determine whether or not using liquid-ammonia as hydrogen storage and electrolyzing it to obtain the hydrogen is a viable hydrogen storage technology compared to the 2010 technical targets set forth by the DOE [10]. Within this context, there are three objectives:

1. Develop an anode and cathode for the AEC. The Electrochemical Engineering Research Laboratory (EERL) at Ohio University, has demonstrated that combinations of Pt and Ir minimized the overpotential of the electro-oxidation of ammonia resulting in a decrease in power consumption during electrolysis compared to other metals such as Ru, Rh, Ni, and combinations thereof [12,22,23].
2. Design and construct a static alkaline ammonia electrolytic cell. An AEC, that separates hydrogen from the cathode from the nitrogen generated at the anode, was constructed.
3. Determine the feasibility of using ammonia for on-board vehicular hydrogen storage. Synergistic analysis was performed on the AEC and PEMFC. This was carried out using polarization techniques allowing for energy consumption and generation data to be obtained.

2. Experimental/materials and methods

2.1. Electrode preparation

Fig. 1 shows the schematic diagram for the preparation of the electrodes. The anode and cathode base were 3.7 cm × 4.7 cm 18 mesh titanium gauze (0.28 mm diameter wire and 100% purity from Alfa Aesar). Ti gauze served as the current collector for the untreated Toray TGP-H-030 (0.11 μm thick and 80% porosity) carbon fiber paper (CFP) catalytic substrate. The gauze and CFP were supported with titanium foil (0.127 mm thick, annealed, and 99% purity from Alfa Aesar). Titanium was chosen due to its chemical resistance to the acidic environment present during electroplating and the alkaline electrolyte used for testing. Ti gauze was placed between two 3.7 cm × 4.7 cm sheets of CFP. Then, the electrodes were pressed and rinsed with acetone to remove any greasy compounds that may have formed during construction. Overall, the active catalytic sur-

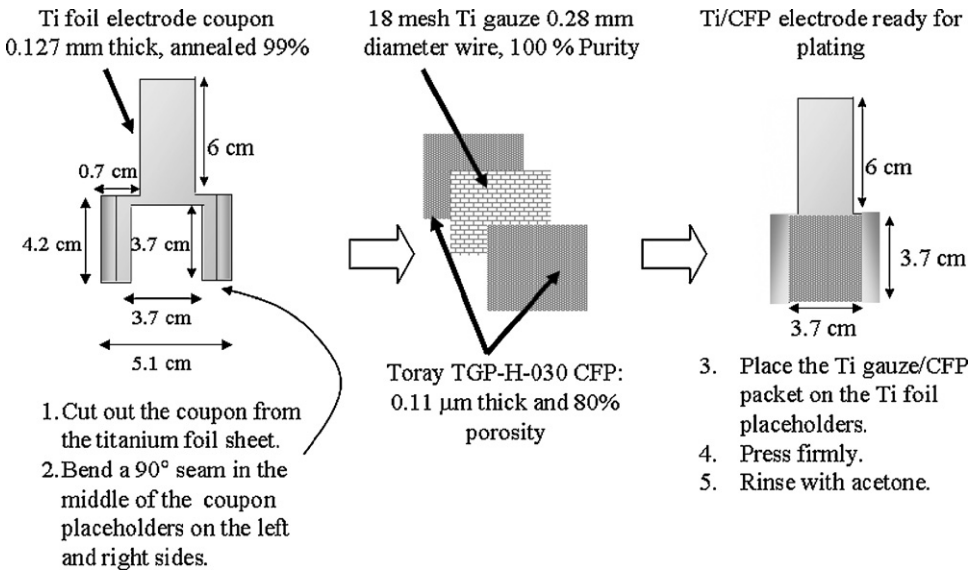

Fig. 1. Schematic representation of the procedure used for the preparation of the carbon fiber paper electrodes. Titanium foil was used as the Ti gauze and CFP support. Ti gauze was used as the current collector to increase the electronic conductivity of the carbon fiber paper.

face area for each electrode was 27.4 cm^2. Finally, the electrodes were dried and weighed before and after electroplating to determine the catalytic loadings.

Electroplating was carried out in a 250 mL beaker that contained 1 M HCl (99.5% pure 6 N from Fisher Scientific) solvated with high performance liquid chromatography (HPLC) water from Alfa Aesar. This solution was temperature controlled at 78 °C with constant stirring at 60 rpm using a 2.5 cm magnetic stir bar. The platinum and iridium salts were dihydrogen hexachloroplatinate (IV) ($H_2PtCl_6{\cdot}6H_2O$—38% Pt) and iridium chloride ($IrCl_3$—55% Ir) from Alfa Aesar, respectively. The purity of both salts was 99.9% (metal basis). Salt concentrations were 2.4 g L^{-1} H_2PtCl_6 and 4.8 g L^{-1} $IrCl_3$. The anode was 4 cm × 4 cm Pt foil (0.102 mm thick 99.95% from ESPI Metals).

The potentiostatic voltage used for plating Pt–Ir was −0.077 V versus Ag/AgCl. It took 1.6 h to deposit 339.4 ± 0.1 mg of Pt–Ir alloy on the anode yielding an average Faradaic plating efficiency of 13.4% based on Pt only since Ir is extremely difficult to deposit alone. Similarly, it took 1.7 h to deposit 355.2 ± 0.1 mg on the cathode with a 12.6% plating efficiency.

Fig. 2 shows scanning electron microscopy (SEM) images of the CFP before plating and anode and cathode CFP after plating. The electrocatalyst loading per mg of geometric surface area was chosen based on the point before the Pt–Ir alloy particles begin to agglomerate and diminish surface area. Fig. 2a is the CFP before plating, Fig. 2b is the anode after plating and after characterizing in ammonia solution (this explains why some of the Pt–Ir deposit has come off in the micro-image), and Fig. 2c is the cathode after plating and testing. On average, the particles ranged between 200 and 300 nm in diameter according to SEM. When electroplating the bimetallic Pt–Ir alloy, the following reductions occur and based on these reduction potentials, iridium can be deposited along with platinum [24,25]. E^0 is referenced to standard hydrogen electrode (SHE):

$$PtCl_6^{2-}(aq) + 4e^- \rightarrow Pt(s) + 6Cl^-(aq) \quad E^0 = 0.744\,V \tag{5}$$

$$Ir^{+3}(aq) + 3e^- \rightarrow Ir(s) \quad E^0 = 1.156\,V \tag{6}$$

The optimum loading of Pt–Ir on this CFP for the electrolysis of ammonia is currently being investigated at the EERL. For the purposes of this paper, 12.4 mg cm^{-2} is an adequate loading ensuring low energy consumption of the AEC.

2.2. Ammonia electrolytic cell design and construction

A sandwich configuration was used for the AEC. Fig. 3 shows the details of the cell design. Main components of the cell are: cast acrylic endplates, ethylene propylene diene monomer (EPDM) rubber gaskets, membrane, and Ti/CFP anode and cathode. These materials were chosen based on their chemical resistance to the alkaline electrolyte present during electrolysis.

Cast acrylic plates (11 cm × 13 cm and 0.95 cm thick) and 0.32 cm thick EPDM (4.7 cm × 4.7 cm) were purchased from McMaster-Carr. A hydrophilic Teflon membrane from W.L. Gore Associates was used as the gas separator. The electrolytic cell was made of a sandwich configuration with the two acrylic endplates holding the electrode/gasket/membrane assembly between them. The cell was tightened ensuring no leaks using stainless steel screw and nuts. Channels (3.175 mm in diameter) were machined at the top of the endplates for the gases to be collected. Also, 8 holes (3.175 mm in diameter) were drilled around the perimeter of the endplates for the stainless steel screws. Since this is a static configuration, there were intermediate bubbles exiting the endplates rather than a continuous flow that a PEMFC desires.

2.3. AEC and PEMFC integration study

In order to determine the feasibility of *in situ* ammonia electrolysis as an on-board hydrogen generating technology, a synergistic analysis of the AEC and PEMFC was required. Fig. 4 shows a schematic representation of the integration experiment. Gas collection columns, which can be seen on the AEC in Fig. 4, were added to both compartments which displace water to the top as the gases exit the AEC; this also pressurizes both compartments equally which allowed the gas to leave the AEC easier. Only one milliliter of hydrogen was required for storage creating a small hydrostatic pressure that helps keep a continuous flow of hydrogen entering the fuel cell. The study was performed using a multi-channel Arbin cycler BT2000. An electrolyte consisting of 5 M KOH was added to the cathode side of the AEC while a solution of 1 M NH_4OH and 5 M KOH was added to the anode. An air-breathable 4 W 5-cell PEMFC from Parker was used.

Before testing, the PEMFC needed to be purged of any air [26]. In order to accomplish this, a simple two-way valve (McMaster-Carr) placed on the hydrogen outlet of the PEMFC was closed.

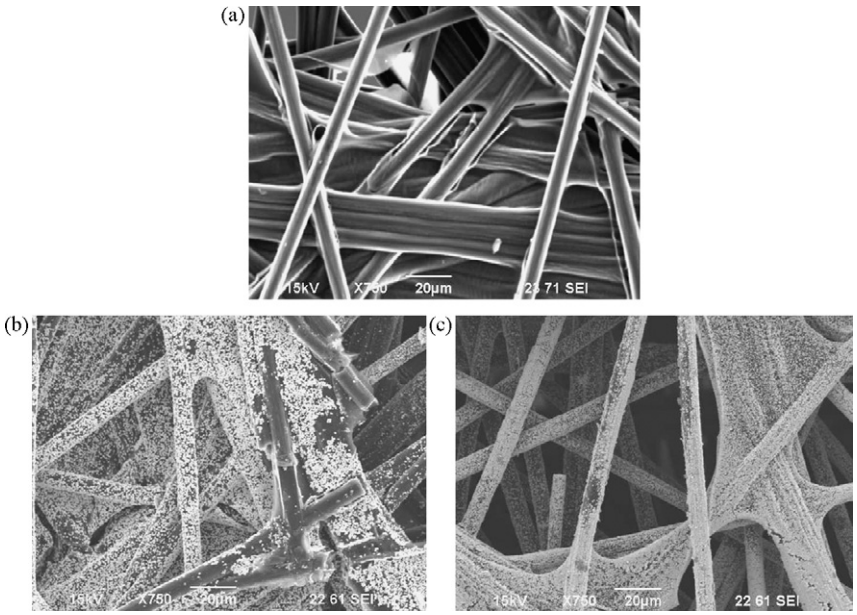

Fig. 2. Scanning electron photomicrographs. Magnification 750×, voltage: 15 kV: (a) Toray TGP-H-030 CFP before plating; (b) anode after plating; (c) cathode after plating.

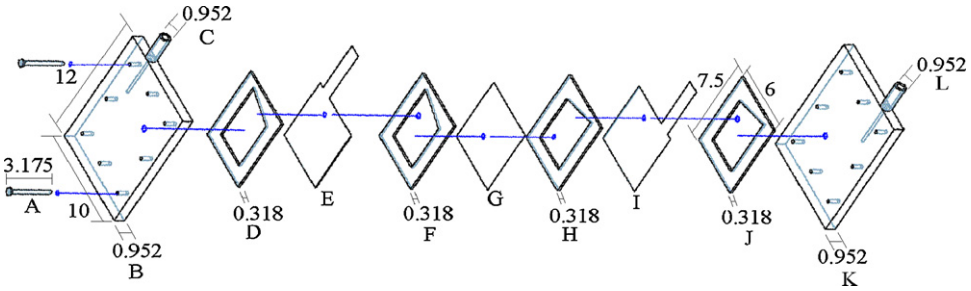

Fig. 3. Schematic representation of the ammonia electrolytic cell (AEC). A sandwich configuration was used, and the parts include: 6-32 stainless steel screws and nuts (A), acrylic plates (B and K), hollow acrylic rods (C and L), ethylene propylene diene monomer (EPDM) gaskets (D, F, H, and J), working and counter electrodes (E and I), and gas separator (G). The channels machined in the acrylic endplates, for both gas collection and holding the cell together using the stainless steel screws, are 0.32 cm in diameter. All dimensions shown are given in cm.

Then, 500 mA was applied to the AEC until 12 mL of hydrogen was produced (10 mL in the gas collection cylinder + 2 mL in the tubing connecting the hydrogen-side of the AEC to the PEMFC). The hydrogen-outlet valve was then reopened purging any air that may have been present in the H_2 gas collection column and PEMFC. Then, the valve was closed again making the proceeding tests dead ended.

For characterizing the PEMFC at various loads to obtain hydrogen consumption rates, 500 mA was applied to the AEC until 12 mL

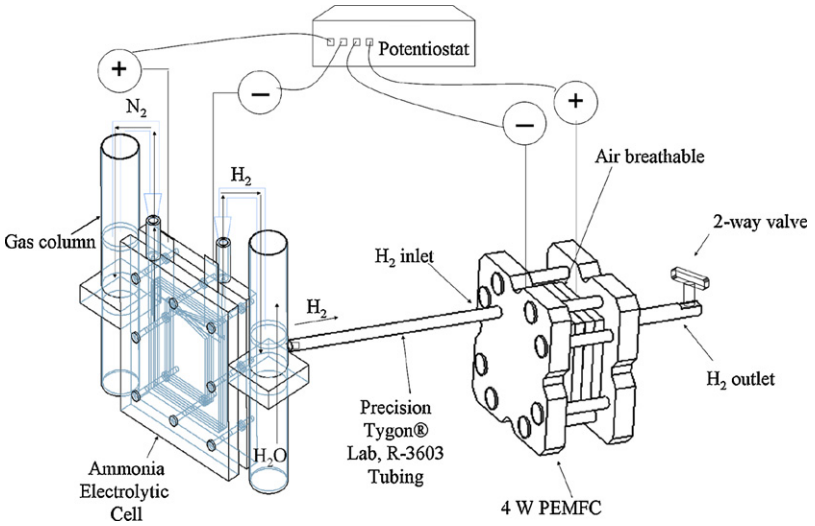

Fig. 4. Schematic diagram of the AEC–PEMFC integration set-up. All integration experiments were performed with this configuration.

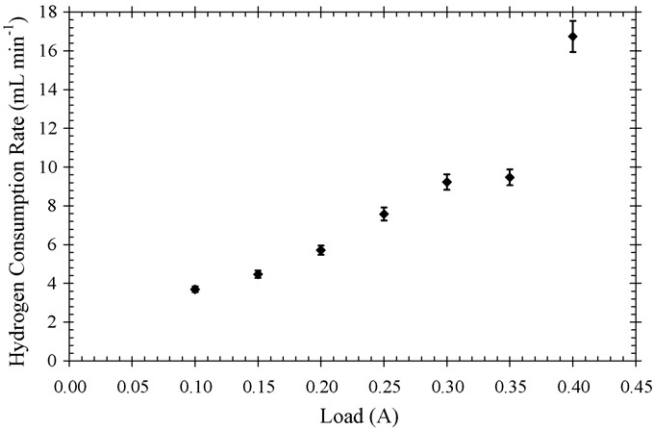

Fig. 5. Hydrogen consumption rates for the PEMFC at various loads using the experimental setup shown in Fig. 4.

of hydrogen was produced and stored. Then the AEC was shut off. Amperic loads ranging from 100 mA to 400 mA in 50 mA increments were applied to the PEMFC individually to determine the hydrogen consumption rate ($mL\,min^{-1}$). Faraday's Law was then used to determine the AEC currents required to generate hydrogen at the same rate of consumption [27]:

$$m = \frac{MIt}{nF} \tag{7}$$

where M is the molecular weight of hydrogen, I is the applied current, t is the time over which the experiment is conducted, n is the number of electrons transferred, and F is the Faradaic constant (96,485 C). Fortunately, ammonia electrolysis has a 100% Faradaic efficiency [12]. So, the currents predicted from Faraday's Law were tested while simultaneously applying the respective loads to the fuel cell to determine if the system could produce hydrogen at the same rate it was consumed. Experiments were performed at 25 °C and 1 atm. Cell potentials for both the AEC and PEMFC were recorded automatically by the potentiostat attaining electric energy consumption and generation data. Based on these data, the feasibility of net energy was determined.

3. Results and discussion

3.1. Integration analysis

Fig. 5 shows the hydrogen consumption rates of the 4 W PEMFC at various loads. The error bars shown were calculated using propagation of error based on the experimental uncertainties of the instrumentation and glassware used.

At a 400 mA load, transport losses dominated. It's important to note that the operating pressure of the hydrogen for the setup in Fig. 4 was atmospheric and less than the manufacturer's suggested 0.14 atm. Table 1 shows the AEC currents required to maintain hydrogen production equivalent to consumption by the PEMFC.

Table 1
AEC currents required to maintain hydrogen production equivalent to consumption.

PEMFC Load (A) ± 0.001	PEMFC Voltage (V) ± 0.0001	Required AEC Current (A) ± 0.001	AEC Voltage (V) ± 0.0001
0.100	4.1632	0.525	0.5232
0.150	3.9642	0.650	0.5564
0.200	3.8931	0.825	0.5877
0.250	3.7804	1.085	0.6274
0.300	3.6511	1.325	0.6659
0.350	3.5120	1.360	0.6824
0.400	2.3532	2.400	0.8450

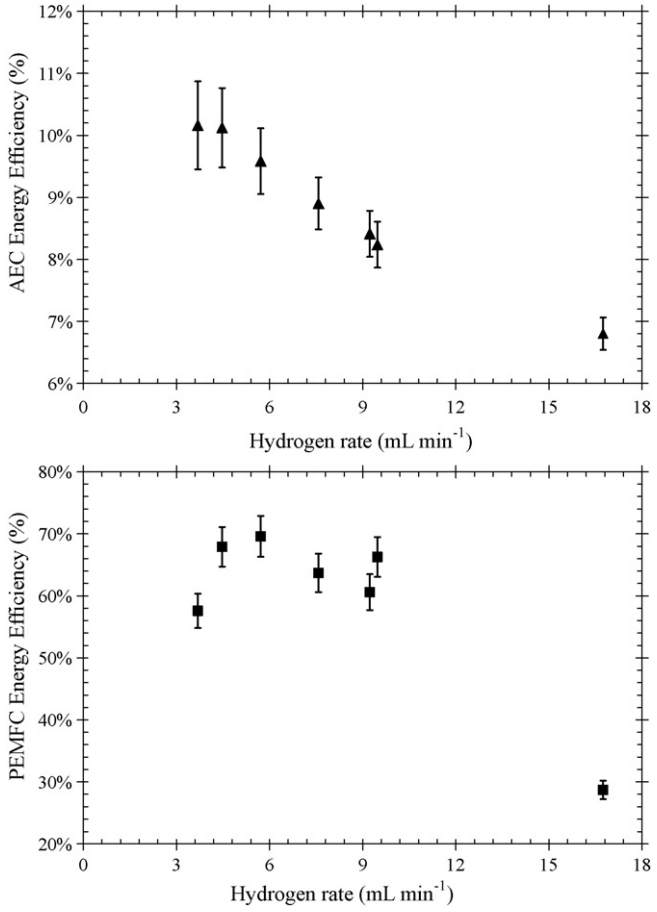

Fig. 6. Energy efficiencies based on thermodynamics at 25 °C: (top) AEC; (bottom) PEMFC.

Fig. 6 shows the energy efficiencies of both the AEC and PEMFC based on thermodynamics. AEC electrical efficiency is low based on the fact that the theoretical energy is only 1.55 Wh g^{-1} H_2 versus the 33 Wh g^{-1} H_2 of hydrogen theoretical energy for PEMFCs.

$$\eta_{AEC} = \frac{\text{Actual Energy Consumption}}{1.55\,\text{Wh}\,\text{g}^{-1}} \tag{8}$$

Fig. 7 shows that the AEC is only consuming 60% of the energy generated from the PEMFC at standard quiescent conditions. It is safe to assume using the heat generated from an electric motor in

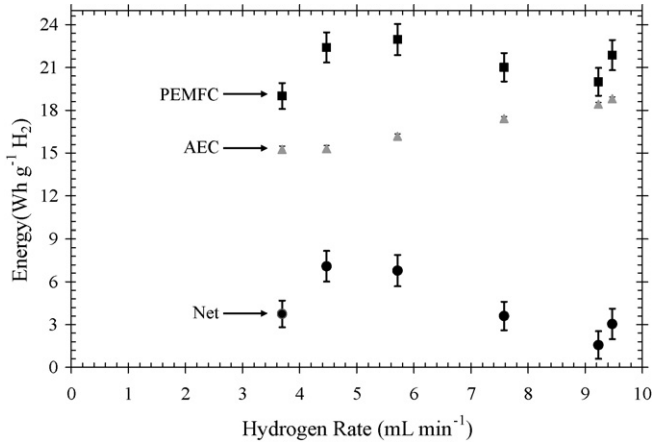

Fig. 7. Net electrical energies from AEC–PEMFC integration analysis preformed at standard conditions.

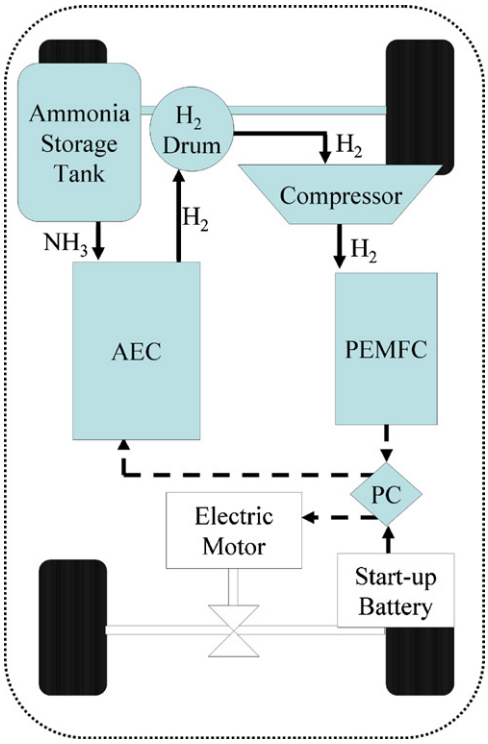

Fig. 8. Schematic representation of an on-board hydrogen storage system using ammonia electrolysis: The components that make up the storage part for this system, which are accounted for when analyzing storage parameters, are: (1) ammonia storage vessel with ammonia fuel; (2) Teflon tubing; (3) ammonia electrolytic cell; (4) start-up hydrogen drum; (5) compressor; (6) PEMFC; and (7) process control.

an automobile in addition to the heat produced from a PEMFC would yield even higher AEC–PEMFC net energies. In order to demonstrate a self-sustaining capability, the hydrogen production rate must equal the consumption rate. Using the PEMFC as air breathable has limitation on the load. According to the manufacturer, 300 mA can be withdrawn before transport losses heavily influence the cell's performance. Due to these transport losses in the fuel cell, a negative net energy ensued while withdrawing 400 mA and was eliminated from Fig. 7. For all the other loads, where transport losses within the PEMFC were not observed, there were net electric energies as high as 9.7 ± 1.1 Wh g^{-1} H_2.

3.2. *Feasibility analysis of ammonia electrolysis as an on-board hydrogen storage system*

Fig. 8 shows a process layout for an on-board hydrogen storage system using ammonia electrolysis. Components of the system which constitute as storage are the ammonia storage tank, AEC, start-up hydrogen drum to maintain a continuous flow of hydrogen to the fuel cell, compressor, PEMFC, process control, and tubing. Other alternative designs that can be optimized to further meet DOE storage parameter targets are possible. These seven major components in Fig. 8 were used to estimate the storage parameters (system gravimetric capacity, system volumetric capacity, and storage system cost) set by the U.S. DOE. This was done to compare ammonia electrolysis storage parameters to the 2010 technical targets set forth by the DOE's FreedomCAR and Fuel Partnership [10]. The results are shown in Table 2.

The following is an individual description of the seven major components required for an ammonia electrolytic process that explains, in detail, the basis for calculating storage parameters. First, liquid ammonia needs to be stored similarly to that of liquid petroleum gasoline [11]. A lightweight and chemical resistant

Table 2
Storage parameters for a HFCV using ammonia electrolysis.

Storage parameter	Units	Ammonia electrolysis	2010 DOE Target
System Gravimetric Capacity	kWh kg^{-1} system kg H_2 kg^{-1} system	1.8 0.09	2.0 0.06
System Volumetric Capacity	kWh L^{-1} system kg H_2 L^{-1} system	1.2 0.059	1.5 0.045
Storage System Cost	US$ $(kWh)^{-1}$ net US$ kg^{-1} H_2	88 1742	4 133
Fuel Cost	US$ gge^{-1} [a] at pump	2.02	2.00–3.00

[a] Gallon of gasoline equivalence (gge).

polymer composite tank from Advanced Lightweight Engineering was used for the design. Second, the tubing to be used is 12.7-cm diameter Teflon tubing from McMaster-Carr. It is approximated that 3 m would be required. Third is the ammonia electrolytic cell. A pump is not required between the storage tank and AEC because the vapor pressure of stored ammonia is high enough to push itself through the electrolyzer. A controller is proposed to manage the amount of ammonia entering the AEC depending on the demand from the PEMFC. It is essentially hydrogen on demand. In addition, since ammonia electrolysis has proven to be 100% efficient, a recycle line of un-reacted ammonia is not required. Fourth, in order for the automobile to be self-sustaining until ammonia is depleted, the fuel cell needs to be powerful enough to run the automobile as well as the electrolyzer. Based on the results shown in Fig. 7, at the highest net energy, the AEC is consuming 60% of the PEMFC's energy. This means that a 69 kW PEMFC is required to meet AEC energy requirements as well as the 483-km range requirement. Fig. 9 shows the energy balance for a HFCV using ammonia electrolysis. Appendix A shows that 41 kW of this PEMFC is used as part of storage based on the fact that the AEC is consuming 60% of the PEMFC's energy. Since the AEC configuration is similar to that of a PEMFC, it was assumed that the AEC weight and volume is approximate to twice the weight and volume of the PEMFC. Once the PEMFC generates enough energy to power the AEC and motor, a start-up battery, used to establish steady state, can be turned off. As a result, this enables a vehicle to be self sustaining and obtain the 483-km range between refueling. Fifth, a start-up hydrogen collection drum will be necessary to ensure the compressor has a continuous flow of hydrogen. A simple high-density polyethylene storage drum from McMaster-Carr was used for storage parameter estimation. Sixth, the compressor weight, volume, and cost were based on the compressor targets in the 2005 *Fuel Cell Technology Road Map* set forth

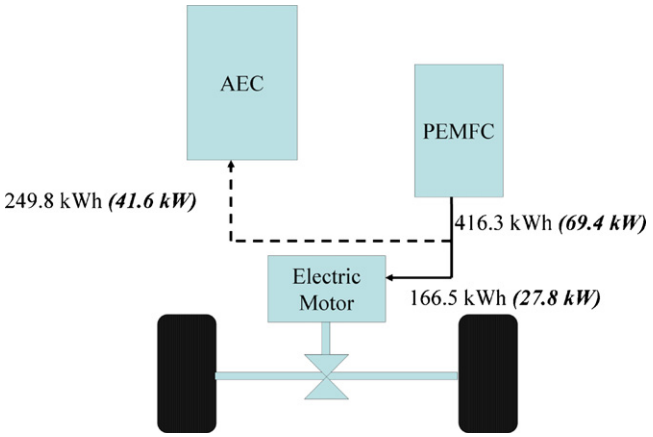

Fig. 9. Balance of plant in terms of energy for a HFCV utilizing *in situ* ammonia electrolysis as hydrogen storage at 25 °C.

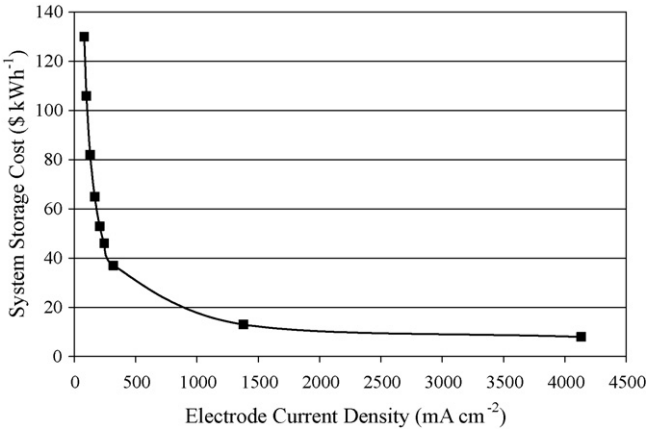

Fig. 10. Sensitivity analysis on the effect of electrode current density and the system storage cost. A steep decent in system storage costs with a small improvement in electrode current density is observed.

by the FreedomCAR and Fuel Partnership [28]. Finally, process control involves taking power from the PEMFC and sending it to the ammonia electrolytic cell and motor. It was determined through AEC and PEMFC synergistic analysis that ammonia electrolysis is most stable at galvanostatic conditions rather than potentiostatatic, so transforming the voltage from the fuel cell to current is necessary. An average engine computer from Autoparts Giant was used to estimate the cost. Details of the calculations and cost analysis can be found in Appendix A.

The weight, volume and cost of 41 kW PEMFC, which is accounted for in the ammonia electrolysis storage system, was determined based on the parameters from the *Fuel Cell Technology Road Map* [29]. When calculating the cost of hydrogen (US$ kg^{-1}), an ammonia cost of 0.36 US$ kg^{-1} was used. This cost would be significantly lower if human and animal waste from domestic wastewater treatment plants and agricultural runoff were used.

In Table 2, despite operating at worst-case conditions (quiescent and room temperature), it appears that ammonia electrolysis as a storage system meets most of the technical targets set forth by the DOE. System gravimetric and volumetric capacities based on energy are lower than the DOE targets because 60% of the PEMFC is accounted for as part of the storage target calculations. On the other hand, the gravimetric and volumetric capacities based on the amount of hydrogen are exceeded. Having a self-sustaining vehicle however makes some of these numbers seem inconsequential. Fig. 10 shows that improving current density of the electrodes significantly decreases the storage system costs. Presently, 130 mA cm^{-2} is achieved; however, if 2,200 mA cm^{-2} were achieved, then the DOE's storage cost for 2010 would be met. Reducing the number of electrodes by increasing the current density will also improve gravimetric and volumetric parameters for using ammonia. There is a linear relationship between the cost of ammonia and cost of hydrogen generated on board as shown in Fig. 11. The cost of ammonia is dependent on the cost of natural gas; however, the cost of ammonia can go as high as 0.53 US$ kg^{-1} before the cost of hydrogen exceeds the DOE target for 2010.

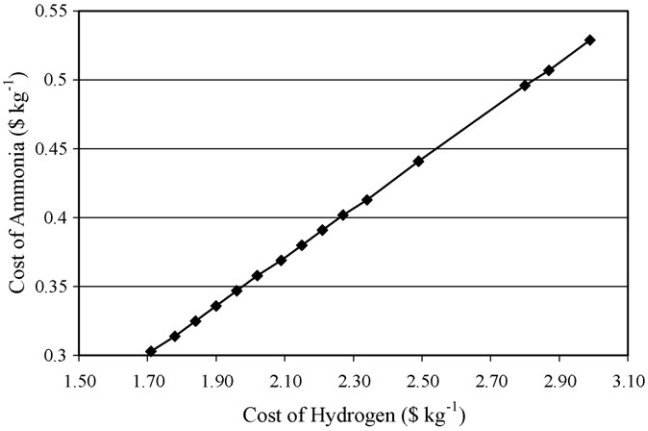

Fig. 11. Sensitivity analysis on the effect of ammonia cost respective to the cost of hydrogen generated on board via ammonia electrolysis.

4. Conclusions

The electrolysis of ammonia was evaluated as a potential technology for the on-board storage and production of hydrogen. Carbon fiber paper was used as catalytic support and Ti foil used as the electrode shell and Ti gauze was used as the current collector. Both anode and cathode were prepared similarly and plated with a Pt–Ir alloy. The electrodes were tested in a sandwich-configured ammonia electrolytic cell (AEC) designed to reduce the ohmic resistance of the cell. A hydrophilic membrane was used to separate the pure gases. Hydrogen generated at the cathode was sent to a 4 W polymer electrolyte membrane fuel cell (PEMFC). Net electric energies were obtained demonstrating the benefit of ammonia electrolysis as an on-board hydrogen storage system. According to scale-up calculations, using an *in situ* ammonia electrolyzer on board will allow a HFCV to travel 483 km between refueling by storing 203 L of aqueous ammonia. At 0.36 US$ kg^{-1} of ammonia, the cost of producing hydrogen on board is 2.02 US$ kg^{-1}.

Appendix A

Storage system costs, gravimetric, and volumetric capacities were calculated using a lightweight 60% peak energy-efficient HFCV that achieves a range of 483 km between refueling.

A.1. Fuel cell power requirement for ammonia HFCV

According to the DOE, a lightweight vehicle achieves 5.3 km L^{-1} and is 2.5 less efficient than a HFCV. A gallon of gasoline is equivalent (gge) to a kg of hydrogen.

$$\text{ICE energy} = 12.5\ \text{gal} \times 33.3\ \text{kWh gal}$$
$$\text{ICE energy} = 416.25\ \text{kWh}$$

$$\text{Amount hydrogen} = \frac{416.25\ \text{kWh}}{2.5 \times 33\ \text{kWh kg}^{-1}} = 5\ \text{kg}$$

In order to travel 483 km with a HFCV, 5 kg of hydrogen is required, which is echoed by the DOE [10]. On average, a car is refueled every 6 h traveling 50 mph. The nominal fuel cell power required to move a lightweight HFCV is:

$$\text{PEMFC power} = \frac{416.25\ \text{kWh}}{6\ \text{h} \times 2.5} = 27.75\ \text{kW}$$

The fuel cell for our system has to be oversized since the ammonia electrolytic cell consumes 60% of the energy. This 60% increase in fuel cell cost, weight, and volume will be declared as part the storage system.

$$\text{PEMFC required} = \frac{27.75\ \text{kW}}{(1 - 60\%)} = 69.38\ \text{kW}$$

A.2. Storage system cost

The ammonia storage vessel, Teflon tubing, centrifugal pump, start-up hydrogen drum, compressor, and controller are common and commercially available equipment. These 6 items are estimated to cost US$ 3200. The AEC and PEMFC cost, weight, and volume are functions of several factors along with several assumptions, and their calculations are shown in detail.

With the increase in power required from the PEMFC comes an increase in the amount of hydrogen required between refueling.

$$\text{Hydrogen} = \frac{69.375\,\text{kW} \times 6\,\text{h}}{33\,\text{kWh}\,\text{kg}^{-1} \times 60\%} = 21.02\,\text{kg}$$

Faraday's Law can be used to predict the current required to produce 21.02 kg (3.5 kg h^{-1}) of hydrogen since ammonia electrolysis is 100% efficient.

$$\text{Current} = \frac{3500\,\text{kg}\,\text{h}^{-1} \times 6\text{e}^{-}\,\text{mol}^{-1} \times 26.8\,\text{Ah/e}^{-}}{3 \times 2\,\text{g}\,\text{mol}^{-1}} = 93,800\,\text{A}$$

Current densities as high as 130 mA cm^{-2} with a cell potential of 0.45 V has been achieved at the EERL with 8.4 mg cm^{-2} Pt–Ir and is currently being improved. With this said, using electrodes with reactive geometric surface areas of 8.1 cm × 7.6 cm creates electrodes with 61.94 cm^2 of surface area. In turn, 8 A can be applied per cell deducing that 11,725 cells are required to obtain 27.2 kW net energy for the motor.

The total catalyst required for the AEC (accounting for anode and cathode per cell):

$$\text{Loading} = 8.4\,\text{mg}\,\text{cm}^{-2} \times 2 \times 11,725\,\text{cells} \times 61.94\,\text{cm}^2 = 12.2\,\text{kg}$$

Assuming that the cost of Ir is equivalent to the cost of Pt, which is expected to cost US$ 900 per troy ounce (2646 US$ kg^{-1}), can be determined. Due to the expense of noble metals, the AEC cost is completely dependent on the loading and catalyst costs meaning that the AEC cost can now be estimated.

$$\text{AEC cost} = 12.2\,\text{kg} \times 2646\,\text{US\$}\,\text{kg}^{-1} = \text{US\$}\,32,281$$

According to Fig. 9, 41.6 kW of the PEMFC are required for storage calculations. Using the 35 US$ kW^{-1} target the DOE has established for fuel cells:

$$\text{PEMFC storage cost} = 35\,\text{US\$}\,\text{kW}^{-1} \times 41.6\,\text{kW} = \text{US\$}\,1456$$

This brings the total system storage cost to US$ 36,937. In terms of the DOE technical storage targets which are summed up in Table 2:

$$\text{Cost 1} = \frac{\text{US\$}\,36,937}{21.2\,\text{kg}\,\text{H}_2} = 1742\,\text{US\$}\,\text{kg}^{-1}$$

$$\text{Cost 2} = \frac{\text{US\$}\,36,937}{33\,\text{kWh}\,\text{kg}^{-1} \times 60\% \times 21.2\,\text{kg}} = 88\,\text{US\$}\,\text{kWh}^{-1}$$

A.3. Gravimetric capacity

The ammonia storage vessel, Teflon tubing, start-up drum, compressor, and process controller are estimated to weigh 26.5 kg based on commercially available products. The weight of fuel, storage part of the fuel cell, and AEC are calculated in detail.

$$\text{NH}_3\,\text{fuel weight} = 21.2\,\text{kg}\,\text{H}_2 \times \frac{1\,\text{kg}\,\text{NH}_3}{0.177\,\text{kg}\,\text{H}_2} = 119.8\,\text{kg}$$

According to Satyapal et al. [10], the target power density for PEMFCs is 2000 W kg^{-1}. As a result, the storage part of the fuel cell will weigh 20.8 kg (41.6 kW ÷ 2(kW kg^{-1})). Using the assumption made earlier that the AEC is twice as heavy as the fuel cell, which is 69.4 kW.

$$\text{AEC weight} = \frac{2 \times 69.4\,\text{kW}}{2\,\text{kW}\,\text{kg}^{-1}} = 69.4\,\text{kg}$$

The total gravimetric capacity is determined using the total estimated storage system weight, which is 236.5 kg.

$$\text{Gravimetric 1} = \frac{21.2\,\text{kg}}{236.5\,\text{kg}} = 0.090$$

$$\text{Gravimetric 2} = \frac{21.2\,\text{kg} \times 33\,\text{kWh}\,\text{kg}^{-1} \times 60\%}{236.5\,\text{kg}} = 1.77\,\text{kWh}\,\text{kg}^{-1}$$

A.4. Volumetric capacity

Similarly, the volumes of the tubing, start-up drum, compressor, and process control are estimated to only occupy 97 L. Using the fact that 119.8 kg of ammonia is required calculated in Appendix A.3. and a density of 682 kg m^{-3}, the storage vessel volume is 174 L. Again, the targeted power/volume density for PEMFCs is 2000 W L^{-1} according to the DOE. Based on the 41.6 kW of fuel cell power that is used for storage, the storage part of the PEMFC requires 20.8 L. Using the 2 times relation for AEC:PEMFC for volume and weight, the AEC occupies:

$$\text{AEC volume} = \frac{2 \times 69.4\,\text{kW}}{2\text{kW/L}} = 69.4\,\text{L}$$

Total storage system volume required is 361.2 L. The volumetric storage parameters are as follows:

$$\text{Volumetric 1} = \frac{21.2\,\text{kg}}{361.2\,\text{L}} = 0.059\,\text{kg}\,\text{L}^{-1}$$

$$\text{Volumetric 2} = \frac{21.2\,\text{kg} \times 33\,\text{kWh}\,\text{kg}^{-1} \times 60\%}{361.2\,\text{kg}} = 1.16\ \text{kWh}\,\text{L}^{-1}$$

References

[1] K. Weissermel, H.J. Arpe, Industrial Organic Chemistry, fourth ed., Wiley, Germany, 2003.
[2] M. Granovskii, I. Dincer, M.A. Rosen, J. Power Sources 157 (2006) 411–421.
[3] M. Granovskii, I. Dincer, M.A. Rosen, J. Power Sources 167 (2007) 461–471.
[4] M.Z. Jacobson, W.G. Colella, D.M. Golden, Science 308 (2005) 1901–1905.
[5] J.J. Hwang, D.Y. Wang, N.C. Shih, J. Power Sources 141 (2005) 108–115.
[6] M.W. Melaina, Int. J. Hydrogen Energy 38 (2003) 743–755.
[7] H.L. MacLean, L.B. Lave, Progr. Energy Combust. Sci. 29 (2003) 1–69.
[8] H.L. Maclean, L.B. Lave, Environ. Sci. Technol. 37 (2003) 5445–5452.
[9] M. Balat, N. Ozdemir, Energy Sources A 27 (2005) 1285–1298.
[10] S. Satyapal, J. Petrovic, C. Read, G. Thomas, G. Ordaz, Catal. Today 120 (2007) 246–256.
[11] G. Thomas, G. Parks, Potential roles of ammonia in a hydrogen economy: a study of issues related to the use of ammonia for on-board vehicular hydrogen storage, U.S. Department of Energy, 2006, p. 23.
[12] F. Vitse, M. Cooper, G.G. Botte, J. Power Sources 142 (2005) 18–26.
[13] G.G. Botte, Carbon fiber-electrocatalysts for the Oxidation of Ammonia, Ethanol, and Coal, and their Application to Hydrogen Production, Fuel Cells, and Purification Processes. U.S., 2004 (patent pending).
[14] G.G. Botte, F. Vitse, M. Cooper, Electrocatalysts for the Oxidation of Ammonia and their Application to Hydrogen Production, Fuel Cells, Sensors, and Purification Processes. U.S. Patent 7,485,211 (2003).
[15] J. Laramine, A. Dicks, Fuel Cell Systems Explained, first ed., J.W. Sons, New York, 2003.
[16] A.F. Bouwman, D.S. Lee, W.A.H. Asman, F.J. Dentener, K.W. VanderHoek, J.G.J. Oliver, Global Biogeochem. Cycles 11 (1997) 561–587.
[17] D.R. McCubbin, B.J. Apelberg, S. Roe, F. Divita, Environ. Sci. Technol. 36 (2002) 1141–1146.
[18] D.C. Bouchard, M.K. Williams, R.Y. Surampalli, J. Am. Water Works Assoc. 84 (1992) 85–90.
[19] S. Basakcilardan-Kabakci, A.N. Ipekoglu, I. Talinli, Environ. Eng. Sci. 24 (2007) 615–624.
[20] K.M. Udert, T.A. Larsen, W. Gujer, Water Res. 37 (2003) 2667–2677.
[21] A. Demirbas, Prog. Energy Combust. Sci. 33 (2007) 1–18.
[22] M. Cooper, G.G. Botte, J. Mater. Sci. Lett. 41 (2006) 5608–5612.

[23] M. Cooper, G.G. Botte, J. Electrochem. Soc. 153 (2006) A1894–A1901.
[24] C.R.K. Rao, D.C. Trivedi, Coord. Chem. Rev. 249 (2005) 613–631.
[25] F. Wu, H. Murakami, Y. Yamabe-Mitari, H. Harade, H. Katayama, Y. Yamamoto, Surf. Coat. Technol. 184 (2003) 24–29.
[26] D.J. Yang, J.X. Ma, L. Xu, M.Z. Wu, H.J. Wang, Electrochim. Acta 51 (2006) 4039–4044.
[27] G. Prentice, Electrochemical Engineering Principles, first ed., Prentice Hall, Saddle River, 1991.
[28] E.J. Carlson, P. Kopf, J. Sinha, S. Sriramulu, Cost analysis of PEM Fuel Cell Systems for Transportation, NREL Subcontract Report SR-560-39104, 2005, pp. 1–109.